Modeling the NO+H 2 reaction on a Pt field emitter tip: Mean-field analysis and Monte Carlo simulations

Y. De Decker, F. Baras, N. Kruse, and G. Nicolis

Citation: The Journal of Chemical Physics **117**, 10244 (2002); doi: 10.1063/1.1518961
View online: http://dx.doi.org/10.1063/1.1518961
View Table of Contents: http://scitation.aip.org/content/aip/journal/jcp/117/22?ver=pdfcov
Published by the AIP Publishing

Modeling the $NO+H_2$ reaction on a Pt field emitter tip: Mean-field analysis and Monte Carlo simulations

Y. De Decker[a)]
Center for Nonlinear Phenomena and Complex Systems, Université Libre de Bruxelles, Campus Plaine, C.P. 231. B-1050 Brussels, Belgium

F. Baras
Center for Nonlinear Phenomena and Complex Systems, Université Libre de Bruxelles, Campus Plaine, C.P. 231. B-1050 Brussels, Belgium and Laboratoire de Recherches sur la Réactivité des Solides, Université de Bourgogne B.P. 47870. 21078 Dijon Cedex, France

N. Kruse
Chemical Physics of Materials, Université Libre de Bruxelles, Campus Plaine, C.P. 243. B-1050 Brussels, Belgium

G. Nicolis
Center for Nonlinear Phenomena and Complex Systems, Université Libre de Bruxelles, Campus Plaine, C.P. 231. B-1050 Brussels, Belgium

(Received 26 February 2002; accepted 11 September 2002)

A minimal model for the $NO+H_2$ reaction on a Pt emitter tip is proposed, with emphasis placed on surface explosions observed in field ion microscopy experiments. The model is first studied in the mean-field approximation, where it is shown to exhibit bistability and associated explosive phenomena. Using kinetic Monte Carlo simulations, irreversible phase transitions, fluctuation-induced dynamics and reaction front propagation are observed, which are not predicted by the mean-field approach. This comparative study allows to shed some light on the origins of the surface explosions, and to investigate the influence of the discrete nature of the support on the dynamics. © *2002 American Institute of Physics.* [DOI: 10.1063/1.1518961]

I. INTRODUCTION

Within the past decades, thanks to the development of sophisticated experimental methods, the investigation of heterogeneous catalytic reactions at the nanoscale has become possible. A rich variety of complex behaviors has in this way been revealed for solid–gas systems, such as organized adsorbate layers, kinetic instabilities, spatiotemporal oscillations, chaos, and so forth.[1] Their occurrence can be traced back to a number of factors characteristic of surface reactions. The strong nonlinearities of the elementary steps involved, the (anisotropic) diffusion of adsorbates at, or beneath, the surface and the global coupling via the gas phase are often invoked.[2] In addition, the lateral interactions between the adsorbed species[3,4] and thermally or adsorbate-induced surface reconstructions[5–8] may play an important role in some systems, especially for the onset of oscillations and the formation of organized phases at the surface. Finally, the spatial constraints induced by the support may also compromise the mixing in the system through the emergence and amplification of inhomogeneous fluctuations, which may lead to fluctuation-induced dynamics.[9–11]

The most familiar description of such processes rests on the mean-field (MF) approximation in the reaction kinetics. It leads to a first understanding of the origin of the nonlinear phenomena, thanks to linear stability and bifurcation analyses. The validity of this description is, however, limited since it cannot take into account the occurrence of inhomogeneous fluctuations. Most catalytic processes actually take place on small particles, exhibiting a restricted amount of active sites for the reaction and where these fluctuations may play a predominant role. Many attempts have thus been made to derive more ''microscopic'' models, reflecting the influence of this restricted geometry of the support on the evolution of the macroscopic variables. Among them, Monte Carlo (MC) simulations applied to surface reactions have witnessed a growing and justified success since the pioneering work of Ziff *et al.*[12] on an irreversible monomer–dimer reaction, mimicking CO oxidation on metal surfaces: the ZGB model. Recent reviews of MC simulations in this field can be found in Refs. 13–15. These simulations are particularly relevant when studying small systems, because they incorporate the discreteness of reactive events in an intrinsic manner. In many instances, a breakdown of the predictions made in the MF description has in this way been brought out.

It is possible for such systems to formally write down a master equation for the probability of a given configuration, which includes local reactive events and can, in principle, lead to the reaction kinetics and spatiotemporal correlations as obtained in the simulations. Unfortunately, exact solutions are rarely attainable as one is generally confronted to an infinite hierarchy of coupled equations for the moments of the underlying probability distribution. Exceptions are provided by very simple reaction schemes (e.g., the monomer–monomer model[16,17]), where this hierarchy may be closed.

a)Electronic mail: Yannick.De.Decker@ulb.ac.be

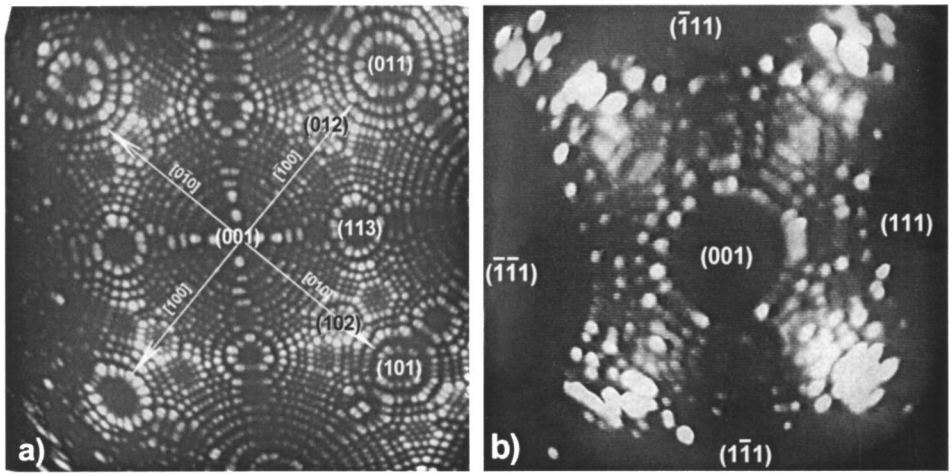

FIG. 1. FIM micrograph (a) of the clean Pt tip (best image conditions in Ne at $F=35$ V nm^{-1}), and the same tip (b) after NO reduction by H_2 ($P_{NO}=2.5\times10^{-3}$ Pa, $P_{H_2}=4\times10^{-3}$ Pa), along with the Miller indices of the most important facets.

More typically, approximate solutions can be found for some systems by truncating the infinite hierarchy to the most relevant moments or by expressing higher moments as functions of lower ones.[18–20] These analytic approaches help to understand how the correlations in the system may lead to the previously mentioned inadequacy of the usual kinetic laws. Still, a full understanding of the differences between MC results and associated MF description is generally lacking. The investigation of this relationship on a minimal model of a real-world complex surface reaction is the principal aim of the present work.

The particular reaction considered is the reduction of nitrogen monoxide (NO) by molecular hydrogen (H_2). This reaction has recently attracted much attention, because of the abundance of nonlinear phenomena associated to it.[1,4,7,21–24] Except for Ref. 24, theoretical investigations mainly focused on the onset of spatiotemporal oscillations and chaos on single crystal surfaces and on the role played by surface reconstruction and lateral interactions in these systems. Our objective here is different. We derive a minimal model for this reaction that retains the main features of the phenomenon as observed by field ion microscopy (FIM) on a Pt field emitter tip,[21] namely the explosive behavior of this reaction. This model allows an analytical treatment, whose conclusions may subsequently be compared to the MC simulations. The experimental results, showing the kinetic instabilities associated with this reaction, are summarized in Sec. II, together with the derivation of the simple model from the full mechanism. In Sec. III, we analyze the behavior of this simplified model in the mean-field description. From the stationary properties, we conclude about the existence of a bistability, that may in turn lead to nontrivial transients in the time evolution for the surface coverages. In view of the small size of the facets where the phenomenon is ignited, we may however question the validity of the MF predictions. To incorporate this size effect as well as the role of the discrete support, Monte Carlo simulations are carried out in Sec. IV. The modifications on the stationary states and the temporal behavior of the system as obtained from these simulations are reported, respectively, in Secs. IV A and IV B, showing the predominant role of poisoning and fluctuations. We also discuss the spatial development of the reaction as deduced from the simulations. Finally, Sec. V is devoted to the main conclusions and perspectives arising from the present work.

II. EXPERIMENTS AND MODEL DERIVATION

A. Experiment

We give here a brief description of the experimental observations underlying the theoretical investigation of this paper. Experiments were performed in a Field Ion Microscope equipped with a video system (time resolution 20 ms) for dynamic studies. For a detailed account of the experimental aspects see Refs. 25 and 26. Pt specimens were prepared in the form of crystal tips using electrochemical methods of thin wire etching.[21] Every Pt tip was characterized for its overall shape and atomic structure before and after the reaction studies. In this manner, it was shown that a Pt tip, subjected to the $NO+H_2$ reaction, may change its original shape from hemispherical to polyhedral. An example of this shape transformation is given in the FIM images of Figs. 1(a) and 1(b) taken with a high-resolution CCD camera.

Running the microscope as a flow reactor with a constant flux of reactant ($P_{NO}=2.5\times10^{-3}$ Pa, $P_{H_2}=4\times10^{-3}$ Pa) at 525 K while imaging at a field strength $F=8.7$ V nm^{-1} led to specific FIM patterns associated with the nonlinear character of the surface reaction. A sequence of such patterns is shown in Figs. 2(a)–2(d). The starting point is an image of moderate brightness in the stepped surface region between the flat (001) pole and the peripheral {111} planes of the pyramidal crystal. In fact, this region of moderate brightness is seen to frame the central part of the crystal which itself appears as a four-leaf cloverlike pattern of low brightness. While this image dominates the video sequence for most of the time, it may suddenly turn into one with superimposed bright areas [Fig. 2(b)]. Subsequently, these areas spread towards the center of the crystal surface so that a crosslike pattern appears in Fig. 2(c). Image brightness fades away in Fig. 2(d) and, finally, the original pattern of Fig. 2(a) is recovered. The process repeats itself in a not strictly periodic fashion. During the dynamic imaging of the $NO+H_2$ reaction, Pt surface atoms arrangements remain invisible. Superimposing Fig. 2(b) on Fig. 1(b) demonstrates, however, that the bright areas correspond to {012} planes, forming the

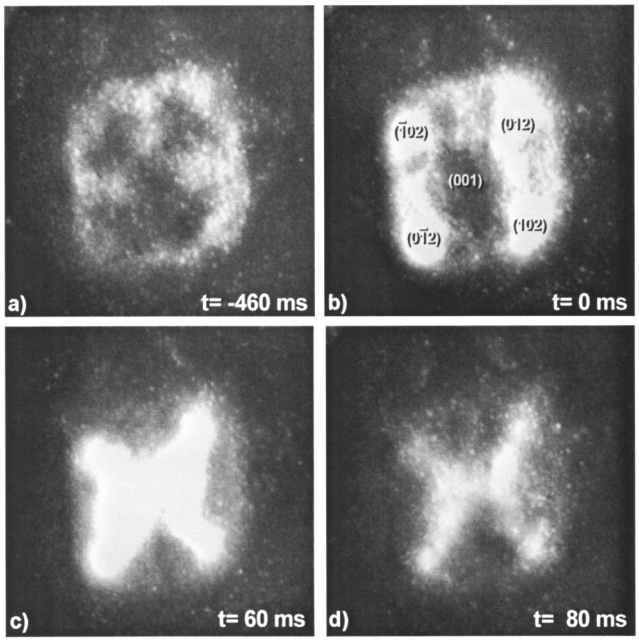

FIG. 2. The sequence of micrographs (a)–(d) illustrates the "surface explosions," with conditions identical to Fig. 1(b) and a field strength $F=8.7$ V nm^{-1}.

corner region of the pyramidal crystal. This assignment does not take into account a possible restructuring of these planes during the reaction.

The sequence of images shown in Figs. 2(a)–2(d) constitutes a catalytic cycle associated with water formation. Obviously, ignition in {012} areas is fast compared with the time resolution (20 ms) of the video system. Instead of igniting sequentially these areas turn bright quasi-simultaneously. Subsequent stages of the cycle comprise front propagation along the [100] zone toward the (001) pole. On the whole, bright patterns disappear after 100–200 ms. Using atom-probe techniques which allow to monitor the local surface composition while imaging (see Ref. 26), it was demonstrated that the imaging species in Figs. 2(a)–2(d) is NO^+. Moreover, after catalytic ignition which is associated with water formation, the NO^+ current was seen to increase drastically and to correlate with bright areas, corresponding thus to a weakly covered surface (where the ionization probability is higher). Note that variable amounts of surface oxygen could also be detected during the reaction.

We finally mention that recent results indicate that these kinetic instabilities are not necessary bound to a pyramidal morphology of the tip.[27] Instead, such phenomena can also be observed on hemispherical crystals. In this case, any surface region along the [100] zone can lead to catalytic ignition, but the associated pattern remains identical.

B. Model

In an attempt to understand the rapid catalytic ignition seen in Figs. 2, an autocatalytic process had been proposed to be in operation,[21] which was based on ideas previously developed by Slinko *et al.*[28] So far, there was no theoretical evidence for the origin of the observed behavior, and, especially, no definitive proof that the kinetics alone could be sufficient for explaining it, without invoking adsorbate-induced surface reconstructions. In order to elucidate this last point, a model for the reaction that retains the main features of the catalytic process needs to be developed on the basis of experimental observations. Neglecting the relatively poor production of NH_x and N_2O compounds (which agrees with atom-probe datas), the surface reaction is expected to proceed according to the following Langmuir–Hinshelwood type mechanism:

$$H_{2(g)}+2S\rightleftharpoons 2H_{(ads)}, \tag{1}$$

$$NO_{(g)}+S\rightleftharpoons NO_{(ads)}, \tag{2}$$

$$NO_{(ads)}+S\rightleftharpoons N_{(ads)}+O_{(ads)}, \tag{3}$$

$$2N_{(ads)}\rightleftharpoons N_{2(ads)}+S, \tag{4}$$

$$O_{(ads)}+H_{(ads)}\rightleftharpoons OH_{(ads)}+S, \tag{5}$$

$$OH_{(ads)}+H_{(ads)}\rightleftharpoons H_2O_{(ads)}+S, \tag{6}$$

$$N_{2(ads)}\rightleftharpoons N_{2(g)}+S, \tag{7}$$

$$H_2O_{(ads)}\rightleftharpoons H_2O_{(g)}+S, \tag{8}$$

where S denotes an empty site on the surface. The subscripts (ads) and (g) are representative of adsorbed and gas-phase species, respectively. In the above scheme, the first two steps correspond to adsorption, steps (3) to (6) refer to the surface reaction itself and desorption is associated with steps (7) and (8). It is possible to further simplify this scheme by assuming that the desorption of both $N_{2(ads)}$ (Ref. 29) and $H_2O_{(ads)}$ is instantaneous (the lifetimes of these species on the surface is very short indeed in the temperature range considered). If, in addition, it is assumed that the $N_{2(ads)}$ and $H_2O_{(ads)}$ formation are fast, steps (3)–(8) can be lumped in the following way:

$$NO_{(ads)}+2H_{(ads)}+S\rightarrow 4S+H_2O_{(g)}+\tfrac{1}{2}N_{2(g)}.$$

This amounts to assuming that the $NO_{(ads)}$ decomposition is the limiting step for the reaction at the surface level. The release of four free sites induces the strong autocatalytic character of the process. Incorporating the above approximations into the full mechanism, reactions (1)–(8) reduce to the simplified scheme

$$H_{2(g)}+2S\underset{k_{-1}}{\overset{k_1}{\rightleftharpoons}}2H_{(ads)}, \tag{9}$$

$$NO_{(g)}+S\underset{k_{-2}}{\overset{k_2}{\rightleftharpoons}}NO_{(ads)}, \tag{10}$$

$$NO_{(ads)}+2H_{(ads)}+S\overset{k_3}{\rightarrow}4S+H_2O_{(g)}+\tfrac{1}{2}N_{2(g)}. \tag{11}$$

There is ample evidence that surface diffusion plays a key role in this system, by allowing coupling between different regions of the tip. In fact, the observation of high NO^+ currents into the {012} surface regions emptied by the catalytic reaction is a clear demonstration for diffusion to occur between facets. In the sequel, however, the model will be studied without explicitly including diffusion, and for the simple case of an isolated (210) facet. We believe that diffusion

principally serves as a means for mass transport toward the active facets. Within each of these facets, the dynamics should be controlled by the kinetic characteristics of the reactive system and not by the diffusion of adsorbates. We will therefore focus on the kinetic origin of surface explosions rather than attempting to reproduce more precisely the observed instabilities, which will be the object of future studies. In particular, our main objective throughout the following sections will be to explore the richness of the simplified model, with emphasis on the potentialities of multistability, that is well-known to induce explosive behaviors. It is thus expected that inclusion of diffusion will not alter qualitatively the results of this paper.

III. MEAN-FIELD BEHAVIOR

The model will first be analyzed in the MF description, and in the limit of a homogeneous system.

The field ion microscope is seen as a flow reactor with constant pressures of nitrogen monoxide (P_{NO}) and molecular hydrogen (P_{H_2}). We are thus dealing with an open reactive system involving adsorbed species $NO_{(ads)}$, $H_{(ads)}$, and empty sites S, which is subjected to nonequilibrium constraints associated with the maintenance of the partial gas pressures.

We suppose that the maximum coverage of the surface corresponds to a monolayer. The partial coverage θ_i of each species must then satisfy the inequalities

$$0 \leqslant \theta_i = \frac{N_i}{N_0} \leqslant 1,$$

where N_i and N_0 are, respectively, the number of adsorbed particles of species i and the total number of available sites. In our case, this implies the following conservation relation

$$\theta_{NO} + \theta_H + \theta_S = 1.$$

The two rate (mean-field) equations associated with this scheme read

$$\frac{d\theta_H}{dt} = 2k_1 P_{H_2}(1-\theta_{NO}-\theta_H)^2 - 2k_{-1}\theta_H^2 - 2k_3\theta_H^2\theta_{NO}(1-\theta_{NO}-\theta_H), \quad (12)$$

$$\frac{d\theta_{NO}}{dt} = k_2 P_{NO}(1-\theta_{NO}-\theta_H) - k_{-2}\theta_{NO} - k_3\theta_H^2\theta_{NO}(1-\theta_{NO}-\theta_H). \quad (13)$$

It is often difficult to experimentally obtain precise values of the kinetic constants involved in elementary steps for surface reactions. Quite often, only qualitative predictions can be made for the rates of the different steps, except for some isolated surfaces. In the case of $NO_{(g)}$ reduction by hydrogen on Pt, values are available for an extended Pt (100) single crystal surface,[4] but to our knowledge not for the {012} facets. To analyze the properties of the model, it is thus convenient to rescale time ($\tau = tk_3$) and to introduce the adimensional parameters

$$P_1 = \frac{k_1 P_{H_2}}{k_3}, \quad P_2 = \frac{k_2 P_{NO}}{k_3}, \quad k_{-1}^* = \frac{k_{-1}}{k_3}, \quad k_{-2}^* = \frac{k_{-2}}{k_3}. \quad (14)$$

For the sake of compactness, we use from now on the notation $\theta_H = x$, $\theta_{NO} = y$, and $\theta_S = 1-x-y = s$ and omit the superscript* for the rescaled desorption kinetic constants. Equations (12)–(13) then become

$$\frac{dx}{d\tau} = 2P_1(1-x-y)^2 - 2k_{-1}x^2 - 2x^2y(1-x-y), \quad (15)$$

$$\frac{dy}{d\tau} = P_2(1-x-y) - k_{-2}y - x^2y(1-x-y). \quad (16)$$

A. Stationary properties

We first consider the limiting case in which the desorption of reactants is neglected ($k_{-1} = k_{-2} = 0$). One sees straightforwardly that Eqs. (15)–(16) admit then the semitrivial steady state solution

$$x_{st} + y_{st} = 1, \quad s_{st} = 0. \quad (17)$$

Since the water production rate is of the form

$$\frac{dH_2O_{(g)}}{d\tau} = x^2y(1-x-y)$$

one concludes that the system becomes totally inactive when it reaches state (17), which corresponds to a lattice poisoned by the two adsorbates $H_{(ads)}$ and $NO_{(ads)}$ in arbitrary proportions. This mixed state is thus infinitely degenerate. Because of this degeneracy, standard linear stability analysis leads to no definitive conclusion, except that poisoning is stable as soon as $P_2 \geqslant 0.444\ldots$.

The remaining (nontrivial) steady states must satisfy

$$x_{st}^3 - \left(1 - \frac{P_2}{P_1}\right)x_{st}^2 + P_2 = 0,$$

$$s_{st} = P_2/P_1, \quad (18)$$

$$y_{st} = 1 - x_{st} - s_{st}.$$

They exist if the following conditions involving the discriminant of the cubic are fulfilled

$$0 \leqslant P_2 \leqslant \frac{4}{27}\left(1 - \frac{P_2}{P_1}\right)^3. \quad (19)$$

Specifically, two nontrivial solutions may appear through a limit point bifurcation for an appropriate choice of the control parameters as given by the right equality in Eq. (19). The stable solution of the pair is representative of a reactive state of the surface which is characterized by a low $NO_{(ads)}$ coverage. Note that the unstable one does not lead to a limit cycle.

Although the system becomes tractable using the above approximation, one cannot definitively conclude on the occurrence of a bistability since the poisoned state (17) is degenerate. Besides, a realistic description must allow for some desorption of at least one of the adsorbed species. In the

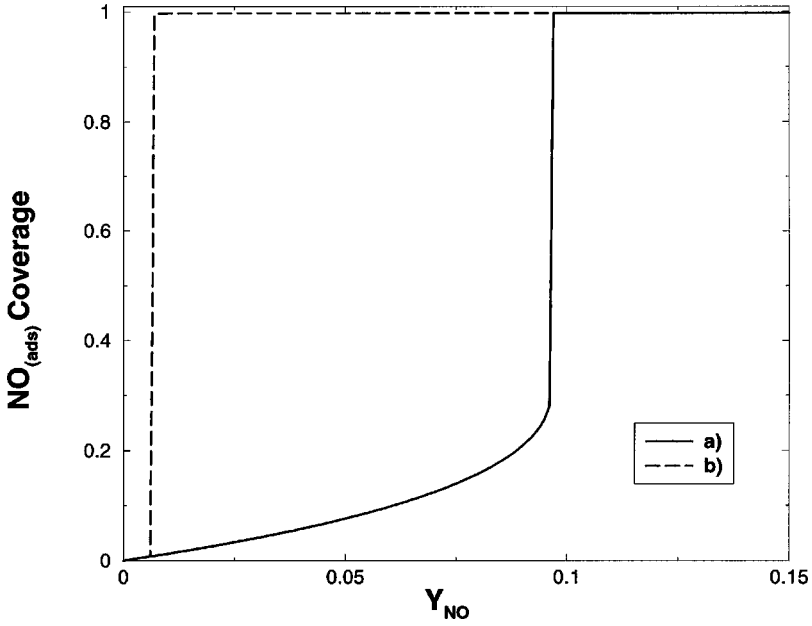

FIG. 3. Steady-state $NO_{(ads)}$ coverage as a function of the partial relative pressure $Y_{NO}=P_{NO}/(P_{NO}+P_{H_2})$ for different initial conditions: (a) $x_0=0.0$, $y_0=0.0$ and (b) $x_0=0.0$, $y_0=0.9$. $k_{-1}=0.01$, $k_{-2}=0.0$.

system considered, the recombinative $H_{(ads)}$ desorption is probably faster than $NO_{(ads)}$ desorption. Unfortunately, respective Temperature Programmed Desorption data for desorption from a Pt (210) single crystal are not available. On a defect-poor Pt (100) surface (subject to a ''hex'' reconstruction in its clean state) major amounts of hydrogen seem to undergo desorption around room temperature, while the onset of $NO_{(ads)}$ desorption is at $\approx$380 K, coinciding with dissociation.[30–33] Setting thus $k_{-1}\neq 0$ in Eqs. (15)–(16), one finds that the semitrivial steady state is now unique and marginally stable. It corresponds to a surface completely poisoned by nitrogen monoxide:

$$x_{st}=0, \quad y_{st}=1, \quad s_{st}=0, \tag{20}$$

while the reactive states satisfy

$$2P_1(x_{st}^2-x_{st}^3-P_2)^2-2P_2x_{st}^2(x_{st}^2-x_{st}^3-P_2)-2k_{-1}x_{st}^6=0, \tag{21}$$

$$y_{st}=P_2/x_{st}^2, \tag{22}$$

$$s_{st}=1-x_{st}-y_{st}. \tag{23}$$

Finding the stationary states associated to Eqs. (21)–(23) via a full analytical treatment is infeasible, since it leads to the resolution of high-degree polynomials. Instead of solving exactly these equations, one can alternatively seek, for small k_{-1}, for perturbative solutions of the stable reactive state in the form

$$x_{st}\approx x_0+k_{-1}x_1 \tag{24}$$

with x_0 being the stationary $H_{(ads)}$ coverage for the stable reactive state in the absence of desorption [solution of the first equation in Eq. (18)]. Substitution of x_{st} from Eq. (24) in (21) leads at the first order to

$$x_1=\frac{x_0^6}{P_1}\left[\left(6-\frac{k_{-1}}{P_1}\right)x_0^5+5\left(\frac{P_2}{P_1}-2\right)x_0^4+4\left(1-\frac{P_2}{P_1}\right)x_0^3+6P_2x_0^2+2\left(\frac{P_2^2}{P_1}-2P_2\right)x_0\right]^{-1}$$

that can be evaluated explicitly. As long as the new stationary state x_{st} possesses the same stability as the reference state x_0, one ends up with a *bistability* between a stable reactive, poorly $NO_{(ads)}$-covered surface and a marginally stable inactive state poisoned by $NO_{(ads)}$. As it will turn out, the very presence of such a bistability plays a central role in the onset of explosive behaviors.

Some remarks should be formulated about the above development. In this approximation, we admit that the values of the coverages for the different species are only slightly displaced in comparison to the values obtained in the total absence of desorption. We also assume that no new stable state arises from the resolution of Eq. (21). This is acceptable only if k_{-1} is small, i.e., the recombinative $H_{(ads)}$ desorption rate must be negligible in comparison to the reaction rate. It might be objected that this is not the case at the high reaction temperatures of the FIM experiments to which we refer. However, the {012} facets expose an open atomic structure with sites likely to provide rather strong binding to $H_{(ads)}$ and $NO_{(ads)}$. Finally, it is also worth noting that the validity of this approach only holds far from the bifurcation, where x_1 diverges.[34]

We now report the results of numerical integration of the evolution equations (15)–(16). This integration fully confirms the existence of bistability with or without partial $H_{(ads)}$ desorption. The associated phase diagram, including recombinative $H_{(ads)}$ desorption, is depicted in Fig. 3 for a particular set of parameters. The constant total adimensional pressure P_1+P_2 is chosen to be equal to 1 and is equivalent to the conditions of MC simulations developed in Sec. IV of

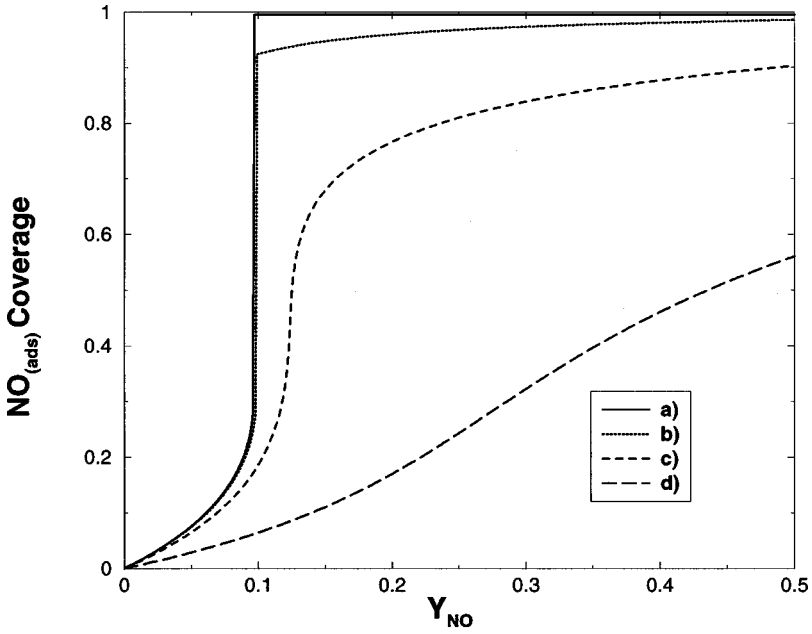

FIG. 4. Steady-state $NO_{(ads)}$ coverage corresponding to the lower branch of the hysteresis loop (Fig. 2), obtained starting from an empty surface, with different $NO_{(ads)}$ desorption rates: (a) $k_{-2}=0.0$, (b) $k_{-2}=0.001$, (c) $k_{-2}=0.01$, and (d) $k_{-2}=0.1$, $k_{-1}=0.01$ in each case (see text).

this paper. As expected from the previous analysis, this diagram is characterized by the presence of a reactive state with low $NO_{(ads)}$ coverage which disappears above a given critical Y_{NO}. This reactive state may coexist with an inactive one, corresponding to a highly $NO_{(ads)}$-covered surface.

The numerical treatment also permits to investigate the influence of increasing H_2 and $NO_{(ads)}$ desorption rates. The results can be summarized as follows: The presence of a bistability is not affected by even very high values of k_{-1}. On the other hand, the bistability between a reactive state and a *nearly* $NO_{(ads)}$-poisoned state is observed for $k_{-2} \leqslant 0.0072$, but is destroyed for higher values (see Fig. 4). Note that we have considered in this latter figure a slight $H_{(ads)}$ desorption in order to avoid problems related to the unrealistic degenerate poisoning. The sensitivity of multistability to monomer desorption in a reactive monomer-dimer model was previously detected for the CO+O_2 reaction, and seems to be a recurrent feature of these systems, even if the reactive step is here quite different. From an experimental point of view, this could provide an interpretation for the observed disappearance of explosive phenomena when the temperature is increased above a critical value.

B. Temporal behavior

An important consequence of bistability is the occurrence of explosive phenomena arising in the vicinity of the turning points of the phase diagram. Indeed, as seen in Fig. 5, for an initially highly $NO_{(ads)}$-covered surface, and for sufficiently low $NO_{(g)}$ relative partial pressures [Y_{NO}

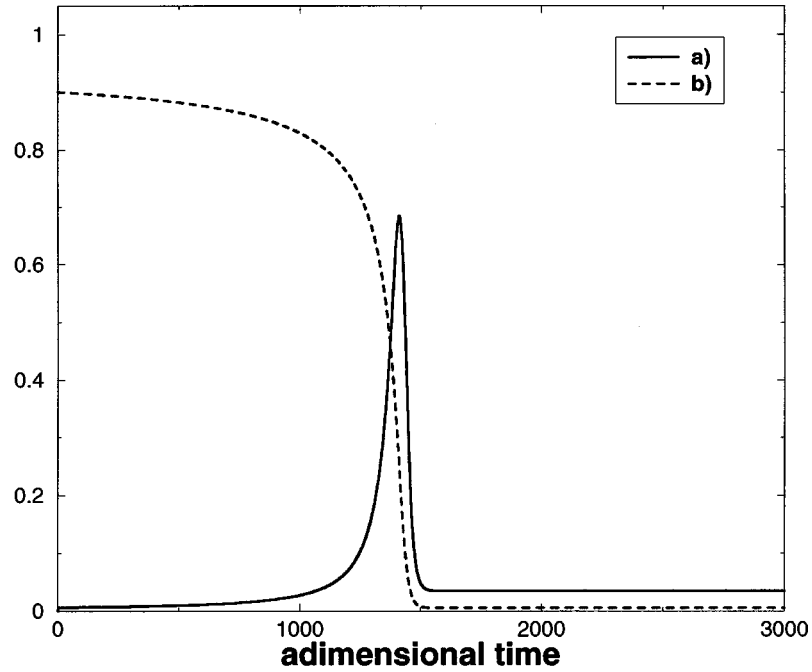

FIG. 5. Temporal evolution for (a) (100×) the water production, given by x^2ys and (b) the $NO_{(ads)}$ coverage y, with $Y_{NO}=0.0005$, $k_{-1}=5.0$, $k_{-2}=0.0$, $x_0=0.0$, $y_0=0.9$. The time scale is in reduced units.

$=P_{NO}/(P_{NO}+P_{H_2})$], the system undergoes a rapid, burst-like transition from a highly $NO_{(ads)}$-covered inactive state, to a less covered, active surface. Since this dynamics is characterized by a sudden increase of both the $H_2O_{(g)}$ production and the number of empty sites, one can easily see that the main features of the phenomena observed on the {012} facets of the FIM experiments are reproduced. Moreover, the pressure conditions qualitatively agree with more recent experimental developments, demonstrating that the catalytic ignition can be found for very low Y_{NO}. Since rate constants are not known explicitly, one cannot however achieve a more precise comparison between MF results and real-world observations. As the onset of the explosive phenomena is intimately related to the presence of the bistability, one expects that they will disappear whenever $k_{-2}>0.0072$ since above this limit, the hysteresis disappears. This is indeed confirmed by numerical investigations.

In contrast to experimental observations, one may notice that only one explosive phenomenon can be seen with a given initial condition. A possible explanation for the occurrence of sustained surface explosions would require the introduction of diffusion, and thus the coupling between facets, which is not considered in the present work. Actually, the {012} facets, where the explosive phenomenon is ignited, are surrounded by facets and rather extended close-packed planes where the $H_{(ads)}$ coverage is most likely to be low (i.e., where $NO_{(ads)}$ dissociation and $H_{2(g)}$ adsorption rates are low). These planes could act as $NO_{(ads)}$ reservoirs, which by diffusion bring back the {012} facet to the high $NO_{(ads)}$-covered state, thereby allowing for another explosive event. This latter effect cannot be taken into account in our simplified view. Other plausible scenarios for the sustained behavior include the role played by fluctuations, or by a slow additional variable, such as the reconstruction of the substrate or the diffusion of adsorbed oxygen atoms in the bulk of the metal. Moreover, it is probable that the dynamics is complicated by the presence of side-reactions, like, e.g., the formation and recombination of hydroxides. Still, the analysis carried out in this section shows that the nonlinearities associated with the chemical mechanisms of the model are sufficient to explain the observed surface explosions.

To identify the effects due to the discrete nature of the support where the reactions actually take place, we now propose to investigate the behavior of the model as obtained by discrete two-dimensional (2D) Monte Carlo simulations.

IV. MONTE CARLO SIMULATIONS

The Monte Carlo algorithm for a 2D lattice can be summarized as follows:

(a) The surface, containing N_0 active sites, is initially filled randomly with a fixed number of $H_{(ads)}$ and $NO_{(ads)}$. The total initial coverage (x_0+y_0) can be less than one, and thus the initial number of empty sites does not have to be zero.
(b) At every Monte Carlo step, one lattice site is chosen randomly.
(c) If this site happens to be empty, $NO_{(ads)}$ adsorption is tried out with a probability equal to the partial pressure of $NO_{(g)}$ (Y_{NO}). If this fails, $H_{2(g)}$ adsorption is attempted with the complementary probability $1-Y_{NO}$, provided that one of the nearest neighbors (NN) of the selected site (taken randomly) is also empty. If no adsorption is possible, 3 NN are chosen randomly. The reaction takes place with a probability of 1, provided that these selected sites are occupied by 2 $H_{(ads)}$ and 1 $NO_{(ads)}$.
(d) If the site is occupied by $H_{(ads)}$, reaction is attempted if three randomly chosen NN present the needed configuration ($H_{(ads)}$, $NO_{(ads)}$, and vacant). Alternatively, if a randomly chosen neighbor is also filled with $H_{(ads)}$ then H_2 desorbs with probability $\tilde{k}_{-1}$.
(e) In the case of a site filled by $NO_{(ads)}$, the reaction occurs provided that two $H_{(ads)}$ and one free site occupy three randomly chosen NN. If this fails to happen, $NO_{(ads)}$ desorption is tried with probability $\tilde{k}_{-2}$.
(f) In all other cases the lattice remains unchanged.
(g) Once a Monte Carlo step is terminated a new step may start.

At every time, each site of the surface is characterized by the local occupation numbers

$$n_{i,j}^{NO};n_{i,j}^{H};n_{i,j}^{S}, \tag{25}$$

where $\{i,j\}$ stands for the discrete coordinates on the lattice. These variables take the value 1 or 0 if the site is occupied or not by the respective species. Clearly, the global coverages are given by

$$\theta_X=\frac{1}{N_0}\sum_{i,j} n_{i,j}^{X} \tag{26}$$

with $X=$NO, H, or S. The following conservation laws are straightforward:

$$n_{i,j}^{NO}+n_{i,j}^{H}+n_{i,j}^{S}=1, \tag{27}$$

$$\theta_{NO}+\theta_{H}+\theta_{S}=1. \tag{28}$$

Note that in the architecture of the above algorithm, we implicitly assume that adsorption prevails on reaction and desorption respectively. In doing this we stipulate a specific microscopic mechanism for the reactive events, which was not the case in the equivalent MF model studied in Sec. III. Since the exact mechanistic details of the reaction steps are not known this cannot be checked experimentally, but one should keep in mind that the proposed algorithm is in fact not universal.

From FIM experiments, we know that the peculiar dynamics we are trying to model finds its origin in the {012} facets of the Pt tip. These surfaces contain only a limited number of active sites (about 30), which are rather ill-defined because of the open structure of the {012} plane. The top layer, however, can be conceived as forming a triangular (6 NN) lattice. To simulate the dynamics on an isolated {012} facet, we shall thus limit our investigations on relatively small lattices, with periodic boundaries. As the simulations show no significant modification between the results on square and triangular lattices, we hereafter focus on the simpler case of a lattice with coordination number 4. Moreover,

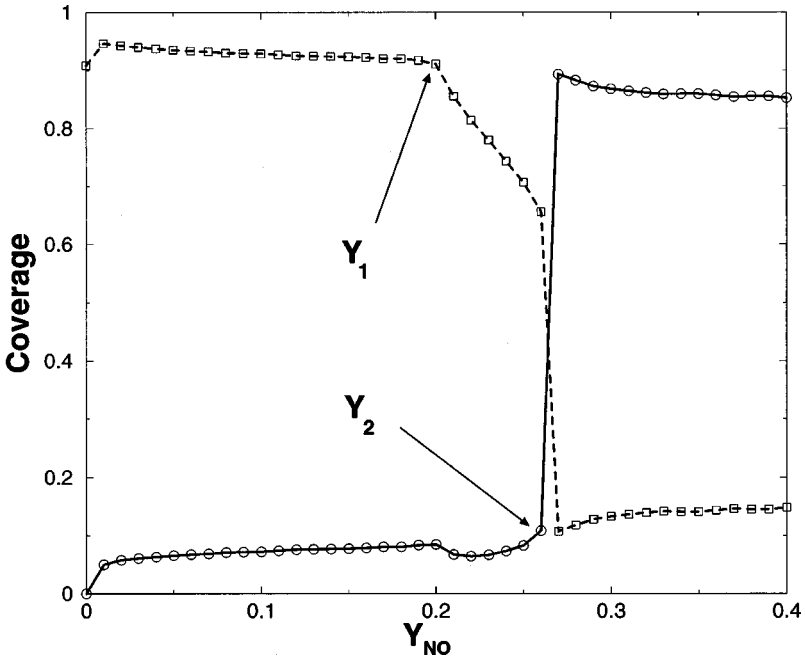

FIG. 6. Steady-state diagram, showing dependence for the coverage of $NO_{(ads)}$ (circles) and $H_{(ads)}$ (squares) in the partial pressure Y_{NO} as obtained by MC simulations on an initially empty surface. $\tilde{k}_{-1}=\tilde{k}_{-2}=0$.

as noticed earlier, we do not consider diffusion of adsorbates in our simulations. This limit is not ''realistic,'' since diffusion of adsorbates is usually fast compared to desorption and reaction, but allows us to emphasize and investigate the role played by the spatial constraints and the unmixing in the breakdown of the MF predictions.

In view of the high molecularity of the reactive step, one could predict that the restricted geometry of the lattice will induce substantial deviations between MF predictions and MC results. To analyze the deviations induced on the values of the steady-state coverages by the spatial constraints of the support, we first focus on the phase diagram. Subsequently, the important role of inhomogeneous fluctuations on the temporal and spatial development of explosive phenomena will be studied.

A. Phase diagram

1. Without desorption

The state diagram in absence of desorption, showing the average (500 realizations) steady-state coverages as a function of the $NO_{(g)}$ partial pressure Y_{NO}, is pictured in Fig. 6.

As Y_{NO} is increased, the system goes from a poisoning zone, corresponding essentially to a $H_{(ads)}$-covered surface, to another poisoned state, associated to a high $NO_{(ads)}$ coverage. Between these two domains ($Y_{NO}\geqslant Y_1\approx 0.20$, and $Y_{NO}\leqslant Y_2 \approx 0.26$), one identifies a ''reactive window'' which is characterized by a high $H_2O_{(g)}$ and $N_{2(g)}$ production rate at the steady state, and by a total coverage $x_{st}+y_{st}\leqslant 1$ (not shown here).

The stationary states of the phase diagram are displaced in comparison to the corresponding MF predictions. For example, the critical value of Y_{NO} signaling in the disappearance of the reactive state, is shifted to higher values. This deviation can be proven to be related to the structure of the Monte Carlo algorithm adopted, and, consequently, to the microscopic mechanism tacitly stipulated. An extended MF description incorporating this mechanism can be set up to explain this deviation. It consists in a single-site approximation of the dynamics, taking into account the structure of the proposed algorithm. The associated results will be presented in detail in a separate publication.

The predominance of poisoned states over the reactive state, now sandwiched between them in a limited zone of the phase diagram, can be understood on the grounds of their absorbing nature on a finite lattice: whenever the system attains transients with a high coverage, a small fluctuation is enough to freeze in a totally poisoned state. Since no desorption can occur, and since empty sites are required for a reactive event, it becomes clear that the system cannot leave this configuration. This effect only occurs for systems in absence of desorption: considering an even slight desorption of $NO_{(ads)}$ will lead, as we will see in the next subsection, to the elimination of this pathologic behavior.

Another important difference between the MC diagram and its MF analogue, is the asymmetry between the behavior of the monomer and dimer species. Unlike the MF case, the $H_{(ads)}$ coverage now undergoes a *smooth* transition between its high and low coverage states. The dependence of the $NO_{(ads)}$ coverage in Y_{NO}, on the other hand, still displays a *sharp* transition, that resembles a first-order kinetic phase transition. This hypothesis may be further confirmed by using the constant-coverage ensemble simulation method developed by Ziff *et al.*,[35] that allows the investigation of unstable steady-states. In this type of simulation, the reaction events remain identical to the classical algorithm, but a constant value for the $NO_{(ads)}$ coverage is imposed. Whenever the coverage takes higher (lower) values than this imposed value, a $H_{2(g)}$ ($NO_{(g)}$) adsorption is tried out, in order to maintain it. The partial $NO_{(g)}$ pressure is then given by the relative amount of $NO_{(g)}$ adsorption trials,

$$Y_{NO}=\frac{\text{number of } NO_{(g)} \text{ adsorption trials}}{\text{total number of adsorption trials}}.$$

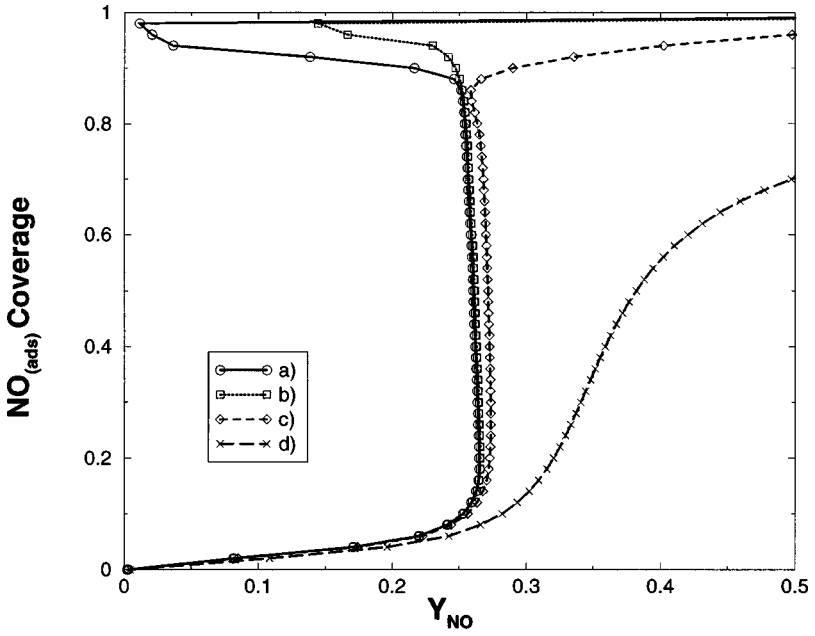

FIG. 7. The $NO_{(ads)}$ coverage of the surface at the steady state, as obtained by the constant-coverage ensemble method (see text). Different desorption probabilities are allowed for $NO_{(ads)}$: (a) $\tilde{k}_{-2}=0$, (b) $\tilde{k}_{-2}=0.001$, (c) $\tilde{k}_{-2}=0.01$, and (d) $\tilde{k}_{-2}=0.1$. Other conditions are identical to Fig. 5.

The fact that an hysteresis can in such a way be obtained for y_{st} [Fig. 7(a)] leads to the conclusion that, in opposition to $H_{(ads)}$, the transition from the low to the high $NO_{(ads)}$ coverage states is first-order. The origin of this difference between the two coverages can be understood qualitatively by the molecularity associated with adsorption in lattice systems: the surface will experience some difficulty to become poisoned by a dimer, while this problem does not arise for the monomer. This dimer-filling problem is especially apparent for the case $Y_{NO}=0$. In these conditions, the system reduces to the classical problem of the random filling of a square lattice by dimer species, here $H_{2(g)}$. This leads to a mean steady-state value $x_{st}=0.9079$, close to the analytical predictions made previously (Ref. 36 and references therein).

2. With desorption

In absence of desorption, the degeneracy of the highly $NO_{(ads)}$-covered state predicted by the MF treatment is still observed. However, in contradiction to the MF predictions, the inclusion of desorption does not lead to the loss of this degeneracy. For recombinative $H_{(ads)}$ desorption alone, the system finally reaches a frozen steady-state, depending on the initial coverage and spatial distribution of the adsorbates. In opposition to the MF predictions, this steady-state still contains $H_{(ads)}$ particles. This is due to the fact that isolated $H_{(ads)}$, embedded in highly $NO_{(ads)}$-covered clusters, may subsist even for very long times since they cannot desorb atomically nor react. In contrast, $NO_{(ads)}$ desorption allows the system to undergo fluctuations even in the presence of a nearly jammed surface. For this reason, in order to avoid unrealistic effects, $NO_{(ads)}$ desorption will always be considered in the following simulations. In accordance with the MF treatment, we must however limit $\tilde{k}_{-2}$ to values lower than a critical value, estimated here as ≈ 0.021. As shown in Fig. 7, higher values for the desorption probability of $NO_{(ads)}$ cause the disappearance of the bistability, and thus of the associated explosive phenomena. We finally mention that, once again, the presence of this bistability is not affected by the $H_{(ads)}$ desorption rate.

One can see in Fig. 8 that including both desorption leads to a state diagram characterized by an enlarged reaction window, and by a slight shift of Y_1 and Y_2 in comparison to the simple case considered in the previous subsection. Note that there still exists a sharp transition in the system between a reactive state to a quasi-inactive state, corresponding here to a *nearly* $NO_{(ads)}$-poisoned surface (complete poisoning is now impossible). In the following section, we shall characterize the stochastic dynamics associated with the transition between these inactive and reactive branches.

B. Dynamics and fluctuations

We now study the effects of intrinsic inhomogeneous fluctuations on the explosive phenomena previously identified in the MF description. Special emphasis will be put on the spatial aspects and their interference with the development of surface explosions.

1. Explosive phenomena

We first analyze some general features of the global explosive behavior corresponding to a single realization. Considering both $H_{(ads)}$ and $NO_{(ads)}$ desorption, leaving thus aside problems related to poisoning of the surface, one ends up with explosive phenomena in the vicinity of turning points. As mentioned above (Sec. III B), transitions from the inactive to the reactive states are of particular interest. Some typical realizations are depicted in Fig. 9 for a 32×32 system. The parametric conditions are such that the system is initially placed near the turning point associated to the disappearance of the inactive state, but outside the bistability region.

Fluctuations induce a wide dispersion in ignition times τ_{ign}, from one realization to another. We observe that τ_{ign} may even become very large (this is reflected by the nonoc-

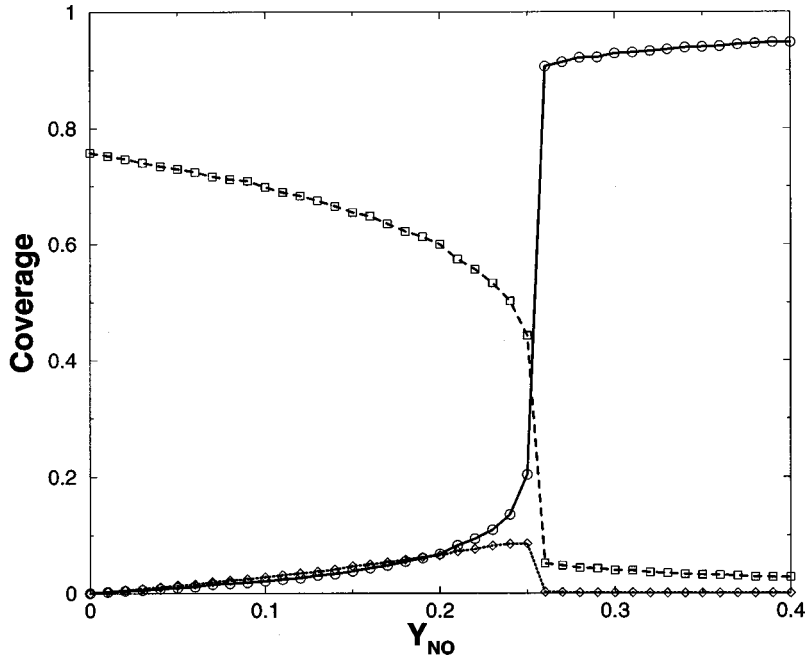

FIG. 8. This diagram shows the stationary $NO_{(ads)}$ coverage (circles), $H_{(ads)}$ coverage (squares), and $H_2O_{(g)}$ produced by time unit and by site (diamonds) when the system admits desorption. Surface is empty in $t=0$, $\tilde{k}_{-1}=0.1$ and $\tilde{k}_{-2}=0.01$.

currence of explosions within the simulation time). The system is thus characterized by a transient bimodality for the distribution of the coverages, in the vicinity of the turning point: for a given time, some realizations correspond to a reactive regime, while the others remain in their initial inactive state. Such a phenomenon has already been predicted in the case of thermal and chemical explosions.[10,11] In agreement with these studies, we observe a broadening of the ignition time distribution as the system evolves closer to the turning point (Fig. 10), where the fluctuations become more important. This fluctuation-induced effect could explain why the explosions observed in the experiments repeat themselves with varying delays in a nonperiodic fashion.

Another fluctuation-induced effect is the appearance of transitions *inside* the bistability. Starting near one of the stable states, the fluctuations can eventually become sufficiently important to induce transitions from an attractor to the other. The occurrence of the explosive phenomena inside the hysteresis can thus be explained by the fact that large amplitude fluctuations in this zone can occur with a nonnegligible probability. It is worth to point out that for the 32×32 system, the state reached *after* the explosion is not subjected to important fluctuations, and thus no reverse transition is observed. A possible explanation for this fact could reside in the different stability properties of the two coexisting states. The situation becomes different when considering very small systems, like, say, a 12×12 square lattice. For such small surfaces, the fluctuations, induced by adsorption-desorption or by reactive events, can become large, and both stable states can undergo strong fluctuations in a common

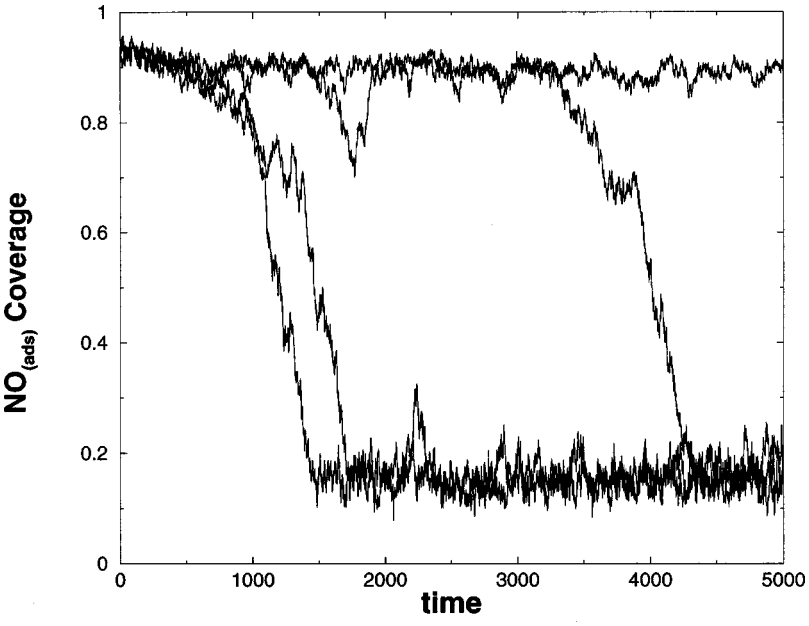

FIG. 9. Time evolution for the $NO_{(ads)}$ covered, starting with a surface highly covered by $NO_{(ads)}$ ($y_0=0.9$, $x_0=0.0$). The partial pressure $Y_{NO}=0.245$, $\tilde{k}_{-1}=0.1$, and $\tilde{k}_{-2}=0.01$.

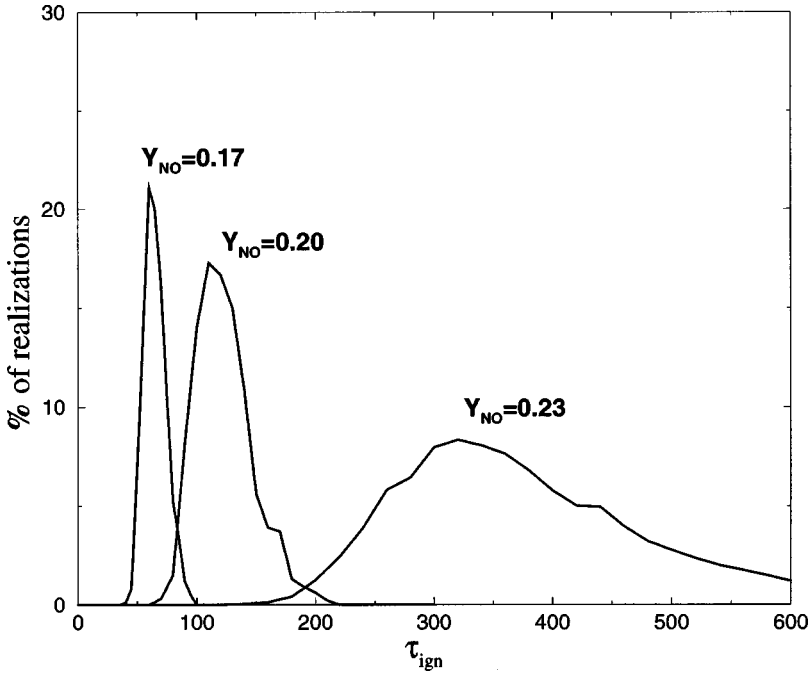

FIG. 10. The distribution of ignition times for the explosions and for different $NO_{(g)}$ partial pressures, obtained from 10 000 realizations. The lattice is initially partially filled by $NO_{(ads)}$ ($y_0=0.8$), the desorption probabilities are the same as that in Fig. 8.

parameter window. The consequence of this latter point is that the system may show, for an adequate choice of the parameters, series of ''flip-flop's'' between the two stable states (Fig. 11). This phenomenon was already reported both in numerical[37] and experimental[9] studies. Finally, we can note that these transitions can be seen if one follows the time evolution in a small window within a much larger system showing itself small fluctuations.

2. Spatial propagation of the explosions

The explosive phenomena considered in the above subsection do not develop homogeneously throughout the system. In Fig. 12, the spatial development of a typical transition (from the inactive to the reactive state) between the two considered states is depicted. For the sake of clarity, a large system is considered here, but the transition mechanism remains identical for smaller surfaces. Starting from a surface mainly covered by $NO_{(ads)}$ species, the system undergoes local composition fluctuations until a sufficiently large cluster of a new ''phase'' is formed. $H_{(ads)}$ and vacant sites are the dominant species in these clusters. This *nucleus* then extends to the whole system, propagating via a pure ''chemical'' front (no diffusion). Propagation is here assured by neighbor-to-neighbor transmission of chemical activity. In a two-dimensional system the number of reactant configurations enabling this propagation is statistically significant, but below some critical dimensionality, such fronts are likely to be

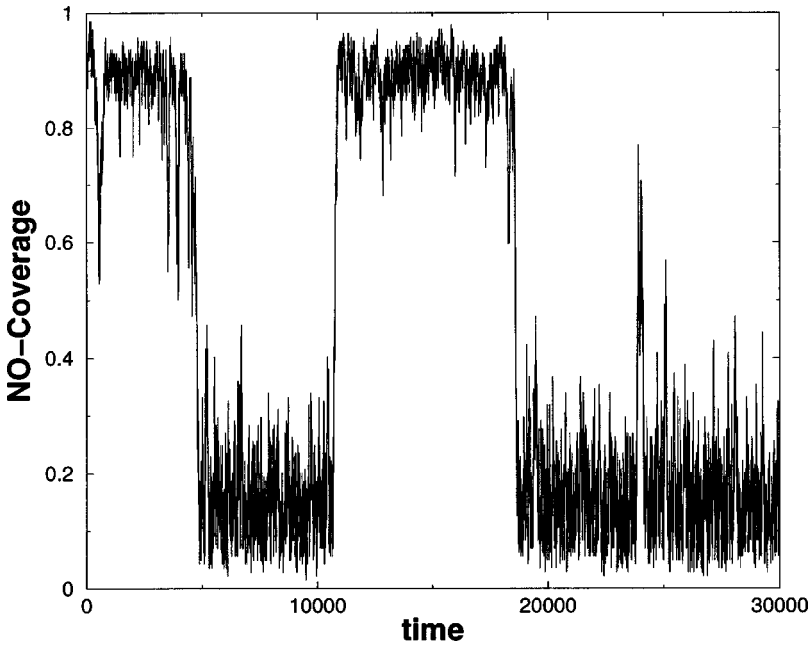

FIG. 11. Behavior of the $NO_{(ads)}$ coverage for the same initial conditions and parameters values as in Fig. 8. The system is now 12×12.

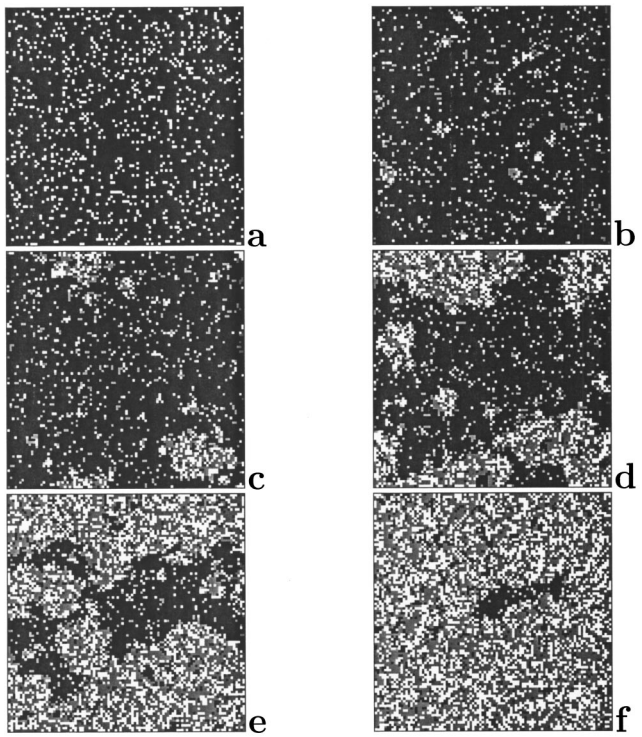

FIG. 12. Spatial development of the surface explosion, for one realization. Conditions identical to Fig. 8, except for the size of the system which is 100×100. Black squares are $NO_{(ads)}$, gray ones are $H_{(ads)}$, and empty sites are blank. Times are respectively 0, 300, 700, 1100, 1500, 1900.

quenched. We realize that this description is qualitative, and the emergence of heterogeneities in the system should be studied in a more rigorous way.

A quantitative characterization of heterogeneities within a system can be obtained by following the time evolution of the global nearest neighbor covariance for a species X, defined as:

$$V^X(t)=\left\langle \frac{1}{L^2}\sum_{i,j}\frac{n^X_{i,j}}{4}[n^X_{i+1,j}+n^X_{i-1,j}+n^X_{i,j+1}+n^X_{i,j-1}]\right\rangle - \frac{1}{L^2}\sum_{i,j}\frac{\langle n^X_{i,j}\rangle}{4}[\langle n^X_{i+1,j}\rangle+\langle n^X_{i-1,j}\rangle+\langle n^X_{i,j+1}\rangle + \langle n^X_{i,j-1}\rangle]. \quad (29)$$

The brackets represent averaging over realizations. An additional spatial averaging is also performed, in order to obtain more efficient statistics. Consider the case of a surface covered by $NO_{(ads)}$. If the system consists at a given time of a unique $NO_{(ads)}$ cluster, occupying the entire surface, clearly $V^{NO}(t)$ must be equal to 0. On the other hand, if $NO_{(ads)}$ particles are separated by more than one site, the first term in Eq. (29) cancels and the covariance takes negative values. Finally, it is easy to check that a configuration of the system where these adsorbates form a large amount of small clusters will lead to positive values for the covariance. $V^X(t)$ is thus representative of the tendency of the X particles to form aggregates of a finite size.

We now consider the evolution of $V^X(t)$ during the explosive transitions between the inactive and active states (surface explosions). As seen in Fig. 13, these explosions are characterized by a transient state where the adsorbed particles are distributed inhomogeneously on the surface, forming a large amount of clusters. One may for example notice that $V^{NO}(t)$ increases although the mean $NO_{(ads)}$ coverage is a decreasing function of time. This directly leads to the conclusion that the transitions imply a nucleation and growth of ''holes'' in a dense $NO_{(ads)}$ phase. From the same figure, we also conclude that these ''holes'' are composed of $H_{(ads)}$ and

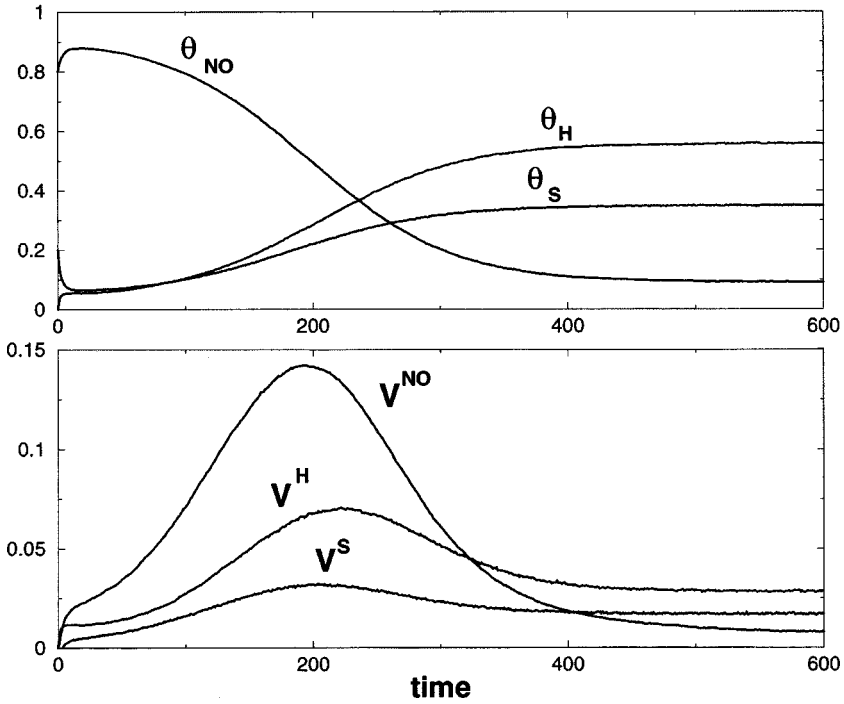

FIG. 13. Time evolution of the coverage and NN covariance $V^X(t)$ for $NO_{(ads)}$, $H_{(ads)}$, and S, obtained from 500 realizations. Conditions are $Y_{NO}=0.22$, $\tilde{k}_{-1}=0.1$, and $\tilde{k}_{-2}=0.01$, $y_0=0.8$, $x_0=0.0$.

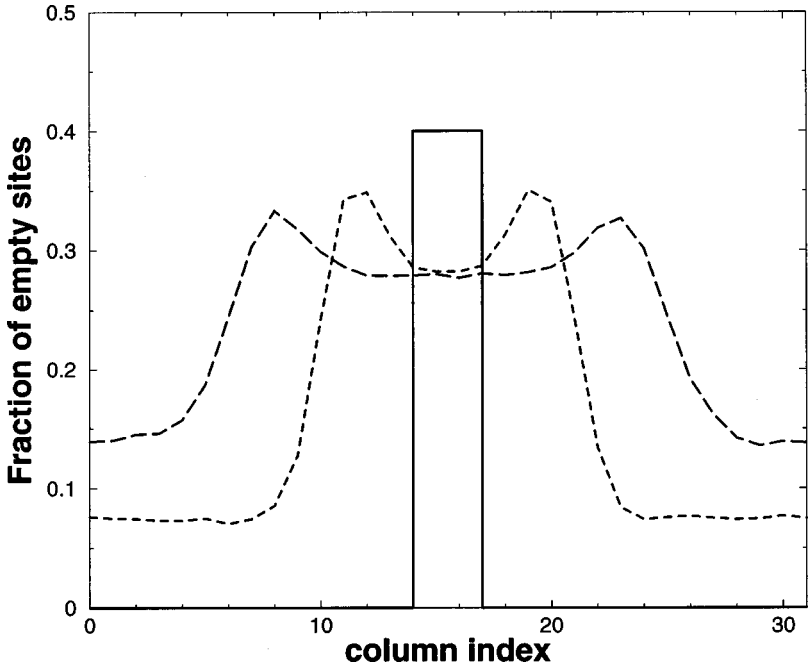

FIG. 14. Spatial propagation of a 4-columns wide reactive cluster into a 32×32 $NO_{(ads)}$-poisoned system, averaged over 500 realizations. The times are 0 (solid line), 20 (dashed line), and 40 (long-dashed line). The cluster is initially covered with $x_0=0.6$ and $y_0=0$. $Y_{NO}=0.1$, $\tilde{k}_{-1}=0.1$, $\tilde{k}_{-2}=0.01$.

S. Such a nucleation and growth mechanism requires the creation of proreactive clusters of a critical size. This induces possibilities of long transients during which the system remains in its initial, unstable dense $NO_{(ads)}$ state, and explains thus in an intuitive way the fact that some of the realizations in Fig. 11 do not lead to a reactive state in the considered time window. On the other hand, transitions from the reactive to the inactive state take place in a homogeneous way and do not involve the specific mechanism of nucleation and growth [$V^X(t)$ is a flat function of time]. The potentialities for observing long transients are thus greatly reduced in comparison to the inverse transitions.

Since no diffusion is included in the simulations at this stage, it is important to investigate the laws governing the propagation of chemical activity pictured in Fig. 12. To this end we prepare the system in a poisoned state, but in a parameter zone where the reactive state is stable ($Y_{NO}=0.1$). A reactive cluster of a sufficient size is deliberately created, that actually consists in a ''reactive band'' with a given width, placed in an otherwise $NO_{(ads)}$-poisoned surface. By further taking the mean coverage on each column of the surface, we reduce the problem to a one-dimensional propagation. The results are rather unexpected (Fig. 14). Not only does the reactive state propagate with a given velocity,[38] but also the interface between the two states has a specific composition: it is a zone mainly composed of empty sites, and where the major part of the $H_2O_{(g)}$ production takes place (not shown here). It can reasonably be expected (and, actually, it has been verified) that mass transfer through conventional diffusion will not alter significantly this result.

This limitation of the reactivity to the boundaries of an expanding state has already been observed in experiments,[39] and could explain the discrepancies of the MF description that are here observed. It is of particular interest for our purposes to point out the interplay between the restricted geometry of the substrate, the high nonlinearity of the reaction and the hard-sphere reactants interactions. This combination is here sufficient to lead to restricted zones of reactivity, and thus to a breakdown of the MF description. This suggests that including diffusion in the system may lead to nontrivial effects because of the low density of the reactive, propagating interface. One may for example imagine that diffusing $NO_{(ads)}$ particles could terminate the propagation of the interface, by invading this region. The spatial mechanism associated to the transitions could thus be modified.

V. CONCLUSIONS AND PERSPECTIVES

We have investigated the behavior of a simple kinetic scheme mimicking the $NO+H_2$ reaction, having as an objective to unravel the origins of observed surface explosions and to understand the role played by the spatial constraints associated with the support. In the MF description, the system gives rise to a bistability between a highly-covered, inactive state and a reactive state associated to a less covered surface. The instabilities observed in the experiments may thus be interpreted as transitions between these two states in the vicinity of one of the turning points. We also showed that the very presence of this bistability is intimately related to the desorption rate of the monomer $NO_{(ads)}$.

The effects of intrinsic, inhomogeneous fluctuations were also studied by means of MC simulations. As it turned out, noise leads to nontrivial effects in the system. First, the steady-states obtained via the simulations show some significant deviations from those arising from the simpler MF point of view. Second, the transient time evolution for the coverages is largely influenced by these fluctuations, and the ignition time for the explosions is seen to be statistically distributed, in qualitative agreement with the experimental observations.

The MC simulations also allowed to study the spatial development of both the explosions and fluctuations in absence of diffusion. The key feature arising from this treatment is the emergence of inhomogeneous transients during the explosive phenomena. This suggests that the explosions consist in a diffusionless nucleation and growth of the reactive state within the inactive one. Moreover, one sees that the reaction is principally localized at the interface between these two ''phases.'' This conclusion is in accordance with experimental[39] and numerical[40] results obtained for other reactive systems on lattice. In opposition to the previous work, we do not have to specifically consider lateral interactions to explain this phenomenon: the hard-core repulsion between adsorbates and the lack of efficient mixing in the system are sufficient.

A natural extension of the present work would be to include diffusion in the simulations. This could lead to significant modifications. The reactive interface referred above is effectively a low-density zone, and diffusion could therefore destroy the spontaneous process of nucleation and growth, leading to an enhanced stability of the inactive state and to a modified spatial propagation. The study of these effects is the subject of further investigations.

The analysis reported in this paper is limited to dynamics on isolated facets. The complex behavior of the system considered is obviously strongly related to the fact that the crystal surfaces used in FIM are composed of many interacting facets, with different size and reactivity. A further development should thus be to model the surface as a patchwork of communicating facets, coupled to each other via diffusion. In this approach one should be able to understand the origins of sustained surface explosions, and the cross-shaped propagation of the observed reaction fronts.

ACKNOWLEDGMENTS

The authors would like to thank T. Visart de Bocarmé and F. Vikas for helpful discussions and support, respectively, in the experimental and computational parts of this study. One of the authors (Y.D.D.) is financially supported by the Faculté des Sciences of the Université Libre de Bruxelles. This work was supported in part by a European Commission DG 12 Grant PSS*1045, by INTAS Grant 577 and by the Communauté Française de Belgique [ARC, No. 96(01-201)].

[1] R. Imbihl and G. Ertl, Chem. Rev. **95**, 697 (1995).
[2] A. S. Mikhailov, Physica A **263**, 329 (1999).
[3] M. Hildebrand and A. S. Mikhailov, J. Phys. Chem. **100**, 19089 (1996).
[4] A. G. Makeev and B. E. Nieuwenhuys, J. Chem. Phys. **108**, 3740 (1998).
[5] R. Imbihl, M. P. Cox, G. Ertl, H. Müller, and W. Brenig, J. Chem. Phys. **83**, 1578 (1985).
[6] V. P. Zhdanov, Surf. Sci. **426**, 345 (1999).
[7] A. G. Makeev and B. E. Nieuwenhuys, Surf. Sci. **418**, 432 (1998).
[8] O. Kortlüke, V. N. Kuzovkov, and W. von Niessen, J. Chem. Phys. **110**, 11523 (1999).
[9] Yu. Suchorski, J. Beben, R. Imbihl, E. W. James, D.-J. Liu, and J. W. Evans, Phys. Rev. B **63**, 165417 (2001).
[10] F. Baras, G. Nicolis, M. Malek Mansour, and J. W. Turner, J. Stat. Phys. **32**, 1 (1983).
[11] P. Peeters, F. Baras, and G. Nicolis, J. Chem. Phys. **93**, 7321 (1990).
[12] R. M. Ziff, E. Gulari, and Y. Barshad, Phys. Rev. Lett. **56**, 2553 (1986).
[13] E. V. Albano, Heterog. Chem. Rev. **3**, 389 (1996).
[14] R. M. Nieminem and A. P. J. Jansen, Appl. Catal., A **160**, 99 (1997).
[15] V. P. Zhdanov and B. Kasemo, Surf. Sci. Rep. **39**, 25 (2000).
[16] E. Clément, P. Leroux-Hugon, and L. M. Sander, Phys. Rev. Lett. **67**, 1661 (1991).
[17] D. S. Sholl and R. T. Skodje, Phys. Rev. E **53**, 335 (1996).
[18] S. Prakash and G. Nicolis, J. Stat. Phys. **82**, 297 (1996).
[19] S. Prakash and G. Nicolis, J. Stat. Phys. **86**, 1289 (1997).
[20] R. Dickman, Phys. Rev. A **34**, 4246 (1986).
[21] C. Voss and N. Kruse, Appl. Surf. Sci. **87/88**, 127 (1994).
[22] N. Khrustova, G. Veser, A. Mikhailov, and R. Imbihl, Phys. Rev. Lett. **75**, 3564 (1995).
[23] P. D. Cobden, C. A. de Wolf, M. Yu. Smirnov, A. Makeev, and B. E. Nieuwenhuys, J. Mol. Catal. A: Chem. **158**, 115 (2000).
[24] G. Kalosakas and A. Provata, Phys. Rev. E **63**, 066126 (2001).
[25] M. Gaussmann and N. Kruse, Catal. Lett. **10**, 305 (1991).
[26] T. Visart de Bocarmé and N. Kruse, Chaos **12**, 1 (2002).
[27] T. D. Chau *et al.* (unpublished).
[28] M. Slinko, T. Fink, T. Löher, H. H. Madden, S. J. Lombardo, R. Imbihl, and G. Ertl, Surf. Sci. **264**, 157 (1992).
[29] The lifetimes of $N_{(ads)}$ and $N_{2(ads)}$ are considered short enough to admit that $N_{(ads)}$ desorbs instantaneously, neglecting second-order molecularity.
[30] H. P. Bonzel, G. Brodén, and G. Pirug, J. Catal. **53**, 96 (1978).
[31] R. J. Gorte, L. D. Schmidt, and J. L. Gland, Surf. Sci. **109**, 367 (1981).
[32] M. A. Barteau, E. I. Ko, and R. J. Madix, Surf. Sci. **102**, 99 (1981).
[33] B. Pennemann, K. Oster, and K. Wandelt, Surf. Sci. **249**, 35 (1991).
[34] A more sophisticated development must then be carried out around the values of both the critical coverage and pressures.
[35] R. M. Ziff and B. J. Brosilow, Phys. Rev. A **46**, 4630 (1992).
[36] J. W. Evans, Rev. Mod. Phys. **65**, 1281 (1993).
[37] K. Fichthorn, E. Gulari, and R. Ziff, Phys. Rev. Lett. **63**, 1527 (1989).
[38] Simulations show indeed that, in average, the interface between the considered states propagates with a constant velocity.
[39] J. Wintterlin, S. Völkening, T. V. W. Janssens, T. Zambelli, and G. Ertl, Science **278**, 1931 (1997).
[40] S. Völkening and J. Wintterlin, J. Chem. Phys. **114**, 6382 (2001).